ARTICLE

Cell-membrane coated iron oxide nanoparticles for isolation and specific identification of drug leads from complex matrices

Received 00th January 20xx, Accepted 00th January 20xx

DOI: 10.1039/x0xx00000x

Jennifer Sherwood, a Josiah Sowell, b Nicholas Beyer, b Jessica Irvin, b Cayman Stephen, b Angelo J. Antone, a Yuping Bao*, a and Lukasz M. Ciesla*, b

The lack of suitable tools for the identification of potential drug leads from complex matrices is a bottleneck in drug discovery. Here, we report a novel method to screen complex matrices for new drug leads targeting transmembrane receptors. Using $\alpha_3\beta_4$ nicotinic receptors as a model system, we successfully demonstrated the ability of this new tool for the specific identification and effective extraction of binding compounds from complex mixtures. The formation of cell-membrane coated nanoparticles was confirmed by transmission electron microscopy. In particular, we have developed a direct tool to evaluate the presence of functional $\alpha_3\beta_4$ nicotinic receptors on the cell membrane. The specific ligand binding to $\alpha_3\beta_4$ nicotinic receptors was examined through ligand fishing experiments and confirmed by high-performance liquid chromatography coupled with diode-array detection and electrospray ionization mass spectrometry. This tool has a great potential to transform drug discovery process focusing on identification of compounds targeting transmembrane proteins, as more than 50% of all modern pharmaceuticals use membrane proteins as prime targets.

1. Introduction

Natural products are rich in bioactive compounds and are considered as a great source of new drug leads. 1,2 Approximately 70% of currently Food and Drug Administration (FDA) approved drugs were first identified in natural products.3 Unfortunately, identification of pharmacologically active compounds from complex samples is very challenging, time consuming, and costly.4 The lack of suitable tools for the identification of potential drug leads from complex matrices is a bottleneck in drug discovery. 1, 4 Even though more than 50% of all modern pharmaceuticals use membrane proteins as prime targets, no effective technology is available so far to enable direct identification of compounds specifically binding to transmembrane proteins with satisfactory outcomes.4 Traditional cell-based assays are not suitable to screen complex mixtures, because they require isolation of individual compounds. $^{4, \, 5}$ High throughput screening techniques used in the majority of modern drug discovery mainly focus on synthetic compound libraries and are not compatible with fishing bioactive compounds from natural resources.² There is a

growing need for innovative tools that can identify potential drug leads in complex mixtures. An ideal approach should preserve natural interactions between transmembrane protein targets and boundary lipids for maintaining the function of transmembrane receptors.6 In addition it should allow for differentiation between specific binding to the targeted transmembrane protein and any type of nonspecific binding.4 It has been previously shown that more targeted, self-designed bioassays accelerate the identification of drug candidates in complex matrices.^{4,5,7-11} For example, cellular membrane affinity chromatography (CMAC) columns have been shown as a valuable tool in drug discovery. 4,5,10,12-15 Immobilization of cellular membrane fragments on immobilized artificial membrane particles has proven to preserve physiological activity of numerous transmembrane proteins.4 Unfortunately, the preparation of the packed column is lengthy, requires large number of cells, and has limited potential for high throughput screening. Magnetic beads with conjugated protein targets have been explored to screen complex matrices for possible new drug leads, however, the conjugated protein targets have been only limited to cytosolic proteins.4,8,11 In addition, magnetic bead-based techniques suffer from significant amount of nonspecific binding due to chemical groups on the bead surfaces. In this paper, we report encapsulation of iron oxide nanoparticles inside vesicles formed by cell membrane fragments with functional transmembrane proteins. The cell membrane fragments help to maintain the function of transmembrane receptors while the full encapsulation of the

^{a.} Chemical and Biological Engineering, University of Alabama, Tuscaloosa, Alabama 35487, United States; e-mail: ybao@enq.ua.edu (Y.B.)

b. Department of Biological Sciences, The University of Alabama, Tuscaloosa,

Alabama 35487, United States; e-mail: $\underline{ImciesIa@ua.edu}$ (L.C.) †Electronic Supplementary Information (ESI) available: HPLC-ESI-MS chromatograms (negative ionization mode) of fishing experiments using CMNPs with $\alpha_3\beta_4$ receptors and artificial mixture [See DOI: 10.1039/x0xx00000x

magnetic nanoparticles prevent the direct interactions between nanoparticles and screening samples, thus minimizing non-specific interactions. The development of this technique is directly benefited from previous studies of using cell membranes encapsulating polymeric nanoparticles for targeted drug delivery and tumour targeting. 16-33

While working on this manuscript, a similar concept was published regarding the development of cell membrane camouflaged magnetic nanoparticles to identify secondary plant metabolites targeting epidermal growth factor receptors.34 Unfortunately, being a concept paper, many key aspects of this technique relevant to drug discovery were not reported, including the confirmation of the presence of transmembrane receptors and evaluation of the binding specificity. Here, using $\alpha_3\beta_4$ nicotinic receptors as a model system, we report the specific identification and effective extraction of binding compounds from complex mixtures using cell membrane coated iron oxide nanoparticles (CMNPs). The formation of CMNPs was confirmed by transmission electron microscopy (TEM). Additionally, the presence of functional $\alpha_3\beta_4$ nicotinic receptors on the cell membrane surfaces was verified by nicotine functionalized nanoparticles. This nanoprobes offers a direct tool to evaluate the presence and binding activity of functional $\alpha_3\beta_4$ nicotinic receptors. These CMNPs were able to specifically fish out binding ligands from artificial and natural mixtures. The binding compounds were identified by highperformance liquid chromatography coupled with diode-array detection and electrospray ionization mass spectrometry (HPLC-DAD-ESI-MS). This tool has a great potential to transform drug discovery process focusing on identification of compounds targeting transmembrane proteins, as more than 50% of all modern pharmaceuticals use membrane proteins as prime targets.

2. Experimental

2.1. Materials

All of the chemical reagents were purchased and used without further purification: chloroform (Sigma-Aldrich, 99%), acetone (BDH, 99.5%), hexane (BDH, 100%), ethanol (BDH, 100%), methanol (Alfa Aeser, 100%), citric acid (CA, Acros, 99.5%), Dulbecco's modified eagle medium (DMEM, ATCC), fetal bovine serum (FBS, Thermo Scientific), penicillin/streptomycin (Thermo Scientific) Tris-HCl, NaCl (>99 %), MgCl₂ (≥ 98%), CaCl₂ (≥ 99%), KCl (>99 %), ammonium acetate (>99 %), benzamidine hydrochloride (>99 %), EDTA (≥ 98%), protease inhibitor cocktail were obtained from VWR. Phenylmethanesulfonyl fluoride (PMSF, ≥ 98.5%), geneticin (G418), nicotine (> 99%) and all other chemicals were purchased from Sigma-Aldrich unless otherwise stated (St. Louis, MO).

2.2. Cell line and cell membrane preparation.

The HEK293 cell line stably overexpressing the human $\alpha_3\beta_4$ nicotinic receptors was obtained from Georgetown University. D-MEM media with 10% Fetal Bovine Serum, 1%

Penicillin/Streptomycin and 0.7mg/ml of geneticin (G418) were used to maintain the $\alpha_3\beta_4$ cells. Cell membranes from the nontransfected HEK-293 cell lines and the transfected $\alpha_3\beta_4$ cell lines were prepared and immobilized following a previously described protocol. $^{5,\,6}$ Briefly, 1 x 10 7 cells were obtained and suspended in 20 mL of Tris-HCl (50 mM, pH 7.4) containing 5 mM EDTA, 100 mM NaCl, 2 mM MgCl $_2$, 3 mM CaCl $_2$, 5 mM KCl, 3 mM benzamidine, 0.1 mM PMSF and 1/100 protease inhibitor cocktail. The suspension was then homogenized using glass Dounce homogenizer, then centrifuged for 5 minutes at 4 9 C at 400 x g. The resulting pellet was discarded, and the supernatant was subsequently centrifuged for 30 minutes at 4 9 C at 100,000 x g. The resulting pellet of cell membrane fragments was used for the preparation of CMNPs.

2.3. Synthesis and functionalization of iron oxide nanoparticles

About 15 nm spherical iron oxide nanoparticles were synthesized using a well-defined thermal decomposition method.³⁵⁻⁴¹ The as-synthesized iron oxide nanoparticles were then functionalized with citric acid (CA) following our wellestablished ligand exchange method. Specifically, citric acid (40 mg, 0.21 mM) dissolved in 0.5 mL of DI water was mixed with 5 mL of nanoparticle chloroform stock solution (1 mg/mL) in 10 mL of methanol and acetone (v/v = 1:1). The reaction mixture was mixed overnight at 45 °C to facilitate the ligand exchange. The CA—functionalized nanoparticles were then collected via centrifugation (15 min, 15,000 rpm) and redispersed in ethanol (5 mL) for a nanoparticle concentration of 1 mg/mL. An equal volume of water was then added, and the solutions were heated up to evaporate the ethanol. The nanoparticles were finally collected via centrifugation and redispersed in water (5 mL).

2.4. Nicotine conjugation and HPLC-MS analysis of nicotine

CA coated NPs were conjugated with nicotine through noncovalent interactions (hydrogen or ionic interactions). For nicotine conjugation, CA-NPs (0.5 mL, pH 7) were simply mixed with 0.5 mg of nicotine overnight at room temperature. To verify the presence of nicotine on the nanoparticle surfaces, freshly conjugated nanoparticles were collected via centrifugation (15,000 rpm, 10 min) and washed 3 times with ammonium acetate buffer (50 mM, pH 7.4) to remove free nicotine. Each wash, the supernatant was collected for analysis. The nicotine labelled nanoparticles were stored in bistris buffer for 5 days prior to their use. The storing buffer was analysed for the presence of nicotine. To elute the nicotine from the nanoparticle surfaces, the final nanoparticle solution was heated in the storing buffer at 60 °C for 15 minutes. In another set of experiments the nicotine labelled NPs were redispersed in phosphate buffer and heated to 60 °C for 15 minutes. The particles were removed using magnet, and the final supernatant was collected and analysed. All the supernatants were analysed for the presence of nicotine using HPLC-MS.

Nanoscale ARTICLE

All the supernatants were analysed using a C18 column (Pursuit C18 250x 4.6 mm, 3 µm) running on an Agilent 1260 Infinity II LC-DAD-MS system using an MSD quadrupole mass spectrometer and an API-ES source. Gradient elution was performed using mobile phases composed of (A) aqueous formic acid [0.01%, v/v] and (B) acetonitrile modified with formic acid [0.01%, v/v] using the following gradient: 2% B from 0 to 5 min; 2% B to 40 %B from 5 to 20 min; 40% B from 20 to 25 min; 40% B to 60% B from 25 to 30 min; 60% B to $98\,\%$ B from 30 to 40 min; 98 % B from 40 to 43 min; 98 % B to 2% B from 43 to 45 min; 2 % B from 45 to 50 min. The mobile phases were delivered at 1 ml/min at room temperature. Detection was accomplished using single ion monitoring in positive ionization mode (m/z 163) with the following settings: drying gas flow at 12 l/min and 350 °C, nebulizer pressure at 35 psig, capillary voltage at 4500 V, fragmentor at 50, gain at 2 and peak width at 0.10 s.

2.5. Formation of CMNPs

CMNPs were formed using cell membranes fragments prepared from non-transfected HEK-293 cell lines and the transfected $\alpha_3\beta_4$ cell lines. The nanoparticles were sterilized in preparation of CMNP formation in 70% ethanol for 15 minutes. The particles were then collected via centrifugation (15 min, 15,000 rpm) and redispersed in sterilized 20 mM bistris (1 mg/mL). To prepare CMNPs, the cell membrane pellet was redispersed in 0.75 mL of autoclaved, 10 mM bistris buffer, and then mixed with 0.25 mL of CA-nanoparticles. The well mixed cell membrane fragments and nanoparticles were incubated on ice for 30 minutes followed by tip sonicating (27% amplitude, 5s on, 5s off). The CMNPs were characterized by transmission electron microscopy (TEM) and dynamic lights scattering (DLS).

The newly synthesized CMNPs containing immobilized nicotinic receptors were then subjected to ligand fishing experiments to prove that the functional transmembrane receptors were immobilized. The CMNPs were submerged in a storing buffer until use in the ligand fishing experiment.

${\bf 2.6. \ Ligand \ fishing \ experiments \ and \ HPLC-DAD-MS \ analysis}$

A 500 μ L equimolar (100 nM) artificial mixture of known nicotinic receptor ligand binders and non-binders was created by mixing 465 μ L of ammonium acetate buffer (pH 7.4, 50 mM) and 5 μ L each of cytisine, berberine, butyrylcholine, anabasine, caffeic acid, nicotine, and warfarin (10 μ M each) solutions. For fishing experiments, CMNPs were separated out of storing buffer with a magnet and the supernatant was discarded. Then, 500 μ L of artificial mixture was mixed with the isolated CMNPs through vortexing and incubated on the rocking rack for 10 minutes to facilitate ligand binding. Then, the CMNPs with bound compounds were isolated from the mixtures with magnets followed by three washes with 500 μ L of ammonium acetate buffer each wash.

After the washes, the bound compounds were eluted three times with 500 μL of elution buffer: first elution, a 9:1 (v/v) solution of ammonium acetate buffer:methanol, second elution, a 9:1 (v/v) solution of ammonium acetate buffer:methanol, and third elution, a 1:9 (v/v) solution of ammonium acetate buffer:methanol. The supernatant of each wash and elution was analysed afterwards using HPLC-ESI-MS technique described in the "Nicotine conjugation and HPLC-MS analysis of nicotine" section of this manuscript.

2.7. Fishing experiments using natural mixture (cigarette smoke condensate)

1 mL of tobacco smoke condensate in acetone was evaporated to dryness under stream of nitrogen. The residue was re-suspended in 1 mL ammonium acetate buffer (pH 7.4, 50 mM) and centrifuged to remove insoluble compounds.

To avoid overloading CMNPs with nicotine an attempt was made to obtain cigarette smoke fraction without nicotine. To this end, 10 μl of cigarette smoke condensate in ammonium acetate buffer was injected 20 consecutive times onto the C18 (Pursuit C18 250 x 4.6 mm, 3 μm) column and a fraction eluting between 6 and 50 minutes was collected and used in fishing experiments. Cigarette smoke condensate in ammonium acetate buffer was fractionated using HPLC gradient described in "Nicotine conjugation and HPLC-MS analysis of nicotine" section of this manuscript. 6-50 min fractions were combined, evaporated to dryness and re-suspended in 500 μL of ammonium acetate buffer.

For fishing experiments, the procedure described in Ligand fishing experiments and HPLC-DAD-MS analysis was used replacing 500 μL of artificial mixture with 500 μL of natural mixture (cigarette smoke condensate).

3. Results and Discussion

The preparation of CMNPs involves several steps (Fig. 1), including (1) preparation of cell membrane fragments with functional transmembrane receptors, which are critical for specific compound binding; (2) synthesis and functionalization of magnetic iron oxide nanoparticles; nanoparticle surface chemistry is important for the formation and stability of CMNPs; (3) preparation of CMNPs; this step must ensure full encapsulation of iron oxide nanoparticles to minimize non-specific binding.

Here, CMNPs were prepared using cell membrane fragments from HEK293 cell line stably overexpressing $\alpha_3\beta_4$ nicotinic receptors. Nicotinic receptors were chosen because they are targets for the development of new drugs for the treatment of numerous diseases, such as nicotine addiction, depression, Alzheimer's disease or chronic pain. Most importantly, Dr. Ciesla has extensive experience in developing and using CMACs with this particular type of receptors. The comparison between the ligand fishing results of these two techniques provides solid validation of this CMNP method.

Cell membrane fragments with functional $\alpha_3\beta_4$ nicotinic receptors were prepared using the previously established protocols. Friefly, 1 x 10⁷ cells were suspended in Tris-HCl buffer (pH 7.4, 50 mM) supplemented with salts and protease inhibitors. The suspension was then homogenized using Dounce glass homogenizer. The mixture was first centrifuged at low speed to remove cell debris and organelles.

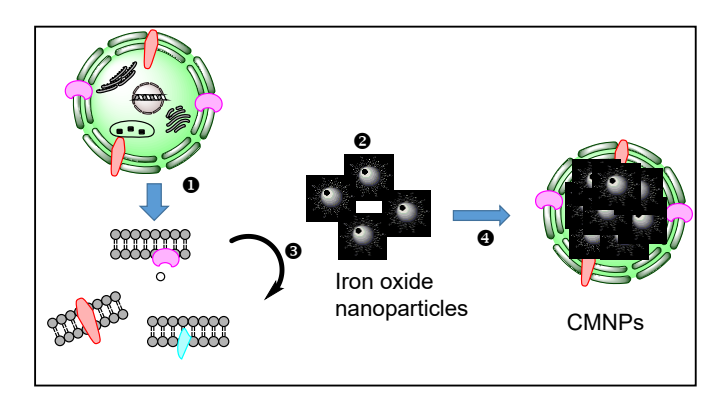


Fig. 1. Overview of CMNP formation: (1) cells expressing targeted proteins, (2) iron oxide nanoparticles, (3) cell membrane fragments obtained after cell lysis, and (4) formation of cell membrane coated nanoparticles.

The remaining supernatant was centrifuged at high speed and the resulting pellet of cell membranes was used to prepare the CMNPs. The synthesis and surface functionalization of iron oxide nanoparticles are well-established in Dr. Bao's laboratory.^{35-37,42,43} Here, we synthesized iron oxide nanoparticles around 15 nm using the modified heat-up method.^{35, 43} Around this size, the nanoparticles are large enough for quick magnetic response and small enough to avoid aggregation due to magnetic interactions.⁴² The surface coatings of the nanoparticles directly interface with the inner parts of the cell membrane fragments, and directly influence the cell membrane coverage. Previous studies on red blood cell membrane coated polymeric nanoparticles suggested that negatively charged surfaces facilitated the cell membrane coverage and positively charged surfaces formed aggregation of cell membrane fragments and nanoparticles.44, 45 Therefore, citric acid (carboxylic groups) was selected as surface coatings for iron oxide nanoparticles, which provide negatively charged surfaces for nanoparticles. Subsequently, these cell membrane fragments and citric acid functionalized nanoparticles were used to prepare CMNPs by an ultrasonication method. In brief, the well-mixed cell membrane fragments and nanoparticles were incubated on ice for 30 minutes followed by ultrasonication (27% amplitude) for 1 minute and 20 seconds (5 s pulse on, 5 s pulse off).

Fig. 2 shows the typical TEM images from CMNPs prepared using the ultrasonication method. Cell membranes and iron oxide nanoparticles have large differences in electron densities and show as different contrasts in TEM images. The membrane shells are light grey circles or barely seen while the iron oxide

nanoparticles are much darker (Fig. 2). Depending on the number of nanoparticles encapsulated inside, some of the CMNPs can be either not spherical or very small sized (Fig. 2a), and higher nanoparticle loading led to the formation of three-dimensional structures (Fig. 2b). For lower nanoparticle loading, the uncontrolled shapes of the CMNPs led to a broad size distribution, as indicated by the DLS plot (Fig. 2c). In contrast, the CMNPs at higher nanoparticle loadings were roughly spherical and exhibited a narrower size distribution (Fig. 2d).

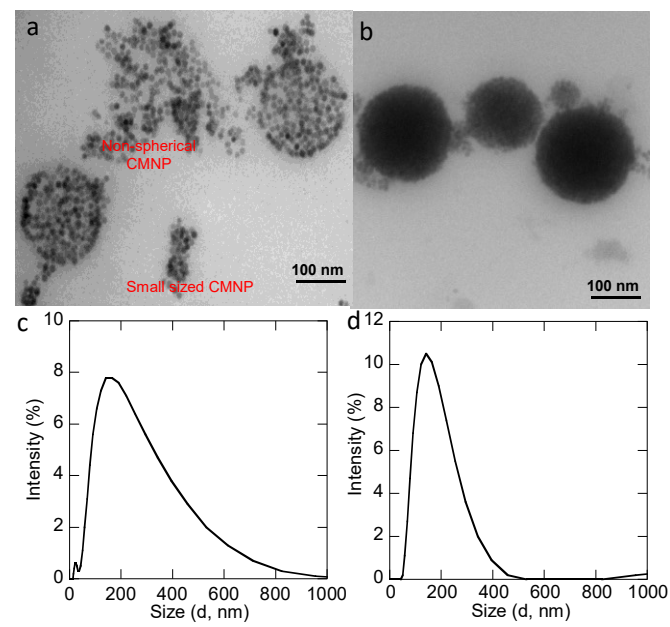


Fig. 2. Typical TEM images of CMNPs: (a) lower nanoparticle loading, and (b) higher nanoparticle loading, (c) DLS plot of lower nanoparticle loading, and (d) DLS plot of higher nanoparticle loading.

The ratio of the cell membrane fragments to iron oxide nanoparticles was estimated by CMNP volume divided by individual nanoparticle volume (Ratio = $\frac{r_{CMNP}^2}{r_{obs}^3}$). Here, the amount of cell membranes was estimated using the HEK 293 cell size (roughly 12 μm in diameter with top and bottom two major surfaces for adhesive cells), cell number (~107), and nanoparticle size (~15 nm). The nanoparticles amount must be smaller than this calculated value to ensure full coverage of the cell membranes. The number of the CMNPs was predicted based on the amount of cell membrane fragments and nanoparticle size. The total cell membrane surface area (A) of 10⁷ number cells was calculated using the following equation: A = $10^7 \times 2\pi R^2$ (R = 6 µm). The TEM image suggested the average size of the CMNPs was around 200 nm in diameter, the rough number of the CMNPs was estimated by $N_{CMNP} = \frac{10^7 x 27}{4 - x^2}$ where r = 100 nm. The number of CMNPs was about $10^{9}-10^{10}$ depending on the membrane recovery. This estimated number of CMNPs in each preparation was used to set up the ligand fishing experiments.

Nanoscale ARTICLE

The presence of functional transmembrane receptors is critical for successful identification of binding compounds during drug screening process. Here, we have developed a novel approach to directly confirm the presence of nicotinic receptors on the CMNP surfaces. Traditionally, the presence of transmembrane receptors is confirmed immunofluorescent staining and microscopy techniques.⁴⁶ While this approach proves the presence of targeted protein, it does not directly confirm functionality of the protein and its ability to specifically bind ligands. To prove the presence of functional $\alpha_3\beta_4$ nicotinic receptors, we have designed nicotinefunctionalized nanoparticles (ligand nanoprobes). The specific interactions between nicotine receptors and nicotine molecules on iron oxide nanoparticles were examined by monitoring the attachment of nicotine-functionalized nanoparticles on the surface of cell membrane vesicles without nanoparticles (empty CMNPs) after incubation. Fig. 3a shows a TEM image of a vesicle prepared from HEK293 cell membrane fragments expressing $\alpha_3\beta_4\,\text{nicotinic}$ receptors (empty CMNPs without encapsulated iron oxide nanoparticles). Without nanoparticles inside, the cell membrane shell is clearly visible. Nicotine-functionalized nanoparticles are seen as black dots, indicating the interactions between nicotinic receptors and nicotine functionalized nanoparticles. We observed no interaction for membrane vesicles prepared with parental cell line not expressing $\alpha_3\beta_4$ nicotinic receptors. We also did not notice interactions between membrane vesicles with nicotinic receptors and nanoparticles without nicotine functionalization.

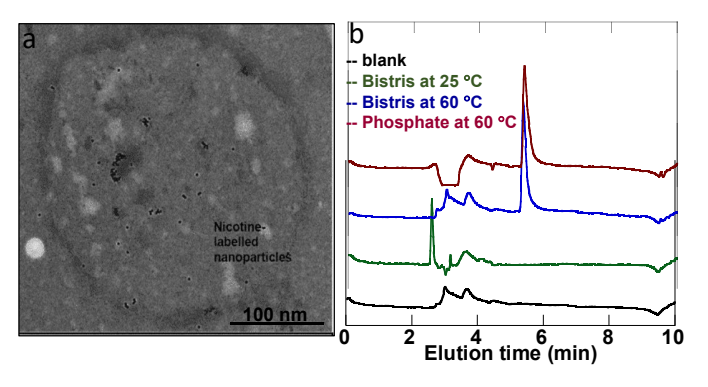


Fig. 3. (a) TEM image of an empty cell membrane vesicle labelled with nicotine functionalized nanoparticles, (b) HPLC-ESI-MS chromatograms (positive ionization mode; m/z 163) of functionalized nanoparticles bistris (storing buffer) at 25 $^{\circ}$ C for 5 days and at 60 $^{\circ}$ C for 15 min and in phosphate buffer at 60 $^{\circ}$ C for 15 min.

The nicotine functionalization on nanoparticle surfaces was achieved through non-covalent interactions (H-bonds and ionic interactions) between citric acid surface coatings and nicotine molecules. The presence of nicotine molecules was confirmed by studying nicotine release from the nanoprobes using HPLC-ESI-MS. Hydrogen or ionic interactions between nanoparticle surface coatings and nicotine were sufficient to form stable nicotine-functionalized nanoprobes. HPLC-ESI-MS analysis of washing and storing buffers for 5 days showed no detectable

amount of nicotine (**Fig. 3b**). Incubation of nicotine-labelled citric acid functionalized nanoparticles at 60 °C in storing bistris buffer or phosphate buffer resulted in the release of nicotine molecules after 15 minutes incubation (**Fig. 3b**).

Neuronal nicotinic acetylcholine receptors (nAChRs) are transmembrane ligand gated ion channels composed of five transmembrane subunits oriented around a central pore. Two families of neuronal transmembrane subunits have been identified, the α subunit family and the β subunit family and these subunits combine to form heteromeric and homomeric nAChRs. Numerous natural alkaloids have been identified as binding and activating nAChRs, for example: nicotine, anabasine or cytisine. Nicotine, and other orthosteric ligands specifically bind in a pocket formed at the interface between the α subunit and the adjacent subunit. The performed experiments showed that nicotine labelled nanoparticles interacted only with empty cell membrane vesicles with nicotinic receptors. This confirms that immobilization results in obtaining functional receptors specifically interacting with its known ligand.

The chracterized CMNPs with functional $\alpha_3\beta_4$ nicotinic receptors were subsequently used for ligand fishing experiments. $10^{9}\sim10^{10}$ CMNPs were mixed with 0.5 mL of artificial mixture containing known binders and nonbinders, followed by incubation at 25 °C for 10 minutes. Then, the CMNPs with bound compounds were isolated from the mixture by a magnet. The separated CMNPs were washed twice with ammonium acetate buffer to ensure removal of compounds with low or no affinity to the nicotinic receptors. The receptor-bound compounds were released during the elution process. The elution process of artificial mixture compounds was monitored using HPLC-DAD-ESI-MS (**Fig. 4**).

The artificial mixture was created with equimolar concentrations (100 nM) of known nicotinic receptor binders: nicotine (#1), anabasine (#2), cytisine (#3) and non-binders: butyrylcholine iodide (#4), berberine (#5), warfarin (#6) and caffeic acid (#7). The artificial mixture was carefully designed to test the ability of CMNPs to selectively "fish out" known binders (protonated alkaloids) from the mixture. Most known binders are compounds with cationic centre, structurally similar to acetylcholine, a compound physiologically binding to nicotinic receptors in human body.47 The design of this artificial mixture containing nonbinders with structural elements similar to binders was critical to test selective binding to CMNP surface receptors. Caffeic acid and warfarin were included in the artificial mixture, because polyphenolic compounds are commonly present in natural mixtures and known to nonspecifically interact with numerous protein targets.

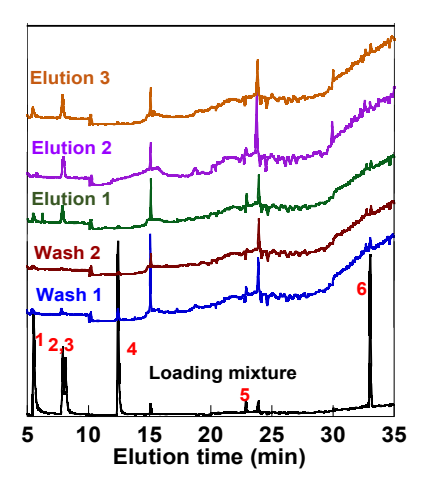


Fig. 4. HPLC-ESI-MS chromatograms (positive ionization mode) of fishing experiments using CMNPs with $\alpha_3\beta_4$ receptors and artificial mixture: washing and elution profiles showing the binding patterns of binders and non-binders. Compounds corresponding with peak numbers are indicated in the text.

Fig. 4 shows the HPLC chromatograms of the screening process. The chromatogram of the loading mixture presents peaks of all the artificial compounds ionizing in the positive mode: nicotine (#1; m/z 163.1; t_R 5.53 min.), cytisine (#2; m/z 191.1; t_R 7.91 min.), anabasine (#3, m/z 163.1, t_R 8.14 min), butyrylcholine (#4, m/z 174.1, t_R 12.43 min), berberine (#5, m/z 337.1; t_R 22.90 min), warfarin (#6, m/z 309.1, t_R 33.08 min). Caffeic acid (#7, m/z 179.1, t_R 16.43) was clearly visible in negative ionization mode (Fig. S1). The peaks of known binders (#1, 2, and 3) were observed in the chromatogram of the first wash but not in the wash 2. The presence of artificial mixture compounds in wash 1 chromatogram was expected, as some remaining traces of loading mixture may still have been present in the analysis tube. The peaks of binders are clearly seen in the elution chromatograms, after the addition of organic modifier. The peak of anabasine and cytysine (# 2 and #3) are higher compared to nicotine peak (#1), which may suggest stronger binding of the latter compounds to the tested nicotinic receptors. The selectivity of the reported drug discovery approach was strongly supported by the absence of butyrylcholine (#4) peak, a compound structurally most similar to a natural ligand acetylcholine indicating the complete removal of nonbinders during washing steps. Two peaks ($t_R \sim 15$ min and 24 min) also clearly seen in all the chromatograms were the noise peaks. Concentration of the ligands released into the washing and elution buffers is relatively low therefore background noise peaks observed in the wash and elution chromatograms seem to be higher compared to noise peaks observed in loading mixture chromatogram (Fig. 4). The background peaks were easily ruled out by running blank samples (buffers) and the peaks did not interfere with the analysis.

The CMNPs were able to selectively retain the known binders (nicotine, anabasine, and cytisine), which were all released during the elution steps (#1, 2, and 3). The absence of

the known non-binders (butyrylcholine, berberine, caffeic acid, and warfarin) in the elution chromatograms suggested their removal during the washing steps. The performed fishing experiments proved the developed nicotinic receptor CMNPs selectively bind known binders without observed binding of different chemical classes of nonbinders.

After proving $\alpha_3\beta_4$ CMNPs can distinguish between known binders and nonbinders in artificial mixture, we further demonstrated the capability of the CMNPs in screening natural mixture for binding compounds. Here, tobacco smoke condensates were used as a model system for the identification of potential $\alpha_3\beta_4$ binding ligands. Cigarette smoke condensates contain high concentration of nicotine which is a known nicotinic receptor ligand. To avoid the overloading of CMNPs with nicotine, we tested smoke cigarette fraction after nicotine removal. The chromatogram of the loading mixture in Fig. 5 shows numerous compounds detected in positive ionization mode. Series of washes with ammonium acetate buffer resulted in the release of compounds with low or no affinity to nicotinic receptors. Subsequent elution steps led to the release of compounds characterized with higher affinity to the CMNP surface receptors. Interestingly, elution 3 chromatogram shows a dominating overloaded peak of nicotine (#1; m/z 163.1; t_R 5.53 min). Traces of nicotine were still present in the loading mixture although the attempt was made to remove this known binder prior to the fishing experiments. The fishing led to nicotine enrichment on the surface of CMNPs and the release of nicotine molecules during elution 3 step is clearly seen in the presented chromatogram (Fig. 5 a). Apart from the nicotine peak, peaks of other compounds were also observed in the elution 3 chromatogram.

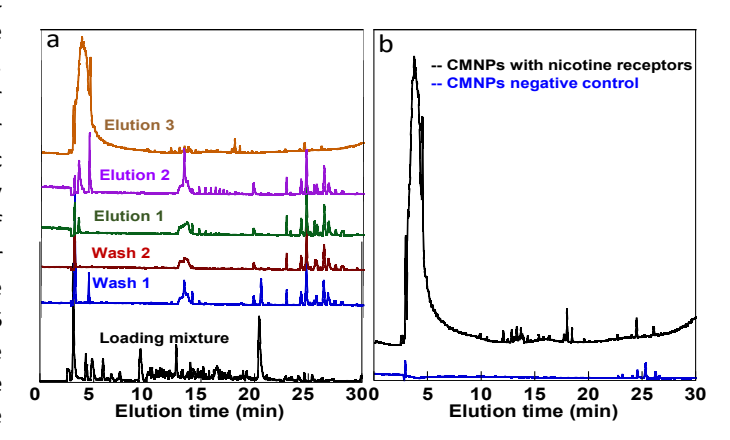


Fig. 5. HPLC chromatograms of fishing experiments using CMNPs with $\alpha_3\beta_4$ receptors and smoke condensates: (a) washing and elution profiles showing the binding patterns of possible ligands, (b) comparison of elution profiles of CMNPs with and without $\alpha_3\beta_4$ receptors.

To rule out binding to targets other than nicotinic receptors fishing experiments were also performed using CMNPs prepared with HEK293 parental cell line not expressing $\alpha_3\beta_4$

Nanoscale ARTICLE

nicotinic receptors as negative control-CMNP(-). Fig. 5b presents elution 3 chromatograms obtained after screening tobacco smoke condensate loading mixture against CMNPs and CMNP (-). Numerous peaks, including the overloaded nicotine peak were present in CMNPs chromatogram but were not observed in CMNP (-) chromatogram. The performed experiments showed that the $\alpha_3\beta_4$ CMNPs were releasing specifically binding compounds after series of buffer washes and elution steps (Fig. 5a). The very same compounds were not binding to CMNPs without nicotinic receptors (Fig. 5 b), proving the specific nature of the observed interactions. We are currently in the process of isolating compounds specifically binding to $\alpha_3\beta_4$ nicotinic receptors and the results will be presented in a separate manuscript. The results obtained with CMNPs were also compared to fishing experiments using previously optimized method CMAC, which provided further validation of the newly developed technique. Data obtained with CMNPs were in agreement with data previously observed using CMAC technique.5

It is worth noting that the reported drug discovery approach focuses on the direct identification of drug leads from natural mixture at the beginning of drug discovery pipeline. Further tests must be performed to verify the pharmacological activities of the binding compounds with other techniques, such as cell-based assays. The direct identification of binding compounds offers an ideal tool to build libraries of natural compounds targeting specific receptors. This is not possible using traditional approach relying on isolation of pure compounds from the analysed mixture, which usually results in studying only most abundant and stable compounds.

4. Conclusions

In summary, we have developed a novel drug discovery assay using $\alpha_3\beta_4$ nicotinic receptors as a model system. We further demonstrated the binding specificity of the CMNPs using both artificial and natural mixtures. These CMNPs were able to selectively fish out binding compounds, such as nicotine, from complex matrices. The proposed assay is fundamentally different from traditional assays in drug discovery, which require pre-defined compound libraries. Therefore, this assay will have a substantial impact on the discovery of new drug leads targeting transmembrane receptors. Even though, the development of CMNPs with nicotinic receptors is discussed in this paper, the assay can be readily adjusted to any other transmembrane protein targets. The applicability of the developed CMNP assay for a variety of transmembrane protein targets will potentially advance multiple drug discovery processes focusing on different transmembrane drug targets. Future studies with this innovative approach will focus on the further optimization of CMNP synthesis and application of this technology for other types of transmembrane receptors.

Conflicts of interest

The authors declare no competing financial interest.

Acknowledgements

This work was supported in part by DMR1149931 (Y.B.) and Alabama Life Research Institute (Y.B. & L.C.). We acknowledge the University of Alabama Department of Biological Sciences for the use of TEM.

Notes and References

- B. Shen, Cell, 2015, 163, 1297-1300.
- A. L. Harvey, R. Edrada-Ebel and R. J. Quinn, *Nat Rev Drug Discov*, 2015, 14, 111-129.
- D. J. Newman and G. M. Cragg, J Nat Prod, 2016, 79, 629-661.
- L. Ciesla and R. Moaddel, Nat Prod Rep, 2016, 33, 1131-1145.
- L. Ciesla, M. Okine, A. Rosenberg, K. S. S. Dossou, L. Toll, I.
 W. Wainer and R. Moaddel, J Chromatogr A, 2016, 1431, 138-144.
- 6. R. Moaddel and I. W. Wainer, *Nat Protoc*, 2009, **4**, 197-205.
- I. Gonzalez-Mariscal, S. M. Krzysik-Walker, M. E. Doyle, Q. R. Liu, R. Cimbro, S. Santa-Cruz Calvo, S. Ghosh, L. Ciesla, R. Moaddel, O. D. Carlson, R. P. Witek, J. F. O'Connell and J. M. Egan, Sci Rep, 2016, 6, 33302.
- 8. M. Rahnasto-Rilla, J. Tyni, M. Huovinen, E. Jarho, T. Kulikowicz, S. Ravichandran, A. B. V, L. Ferrucci, M. Lahtela-Kakkonen and R. Moaddel, *Sci Rep*, 2018, **8**, 4163.
- M. K. Rahnasto-Rilla, P. McLoughlin, T. Kulikowicz, M. Doyle, V. A. Bohr, M. Lahtela-Kakkonen, L. Ferrucci, M. Hayes and R. Moaddel, *Mar Drugs*, 2017, 15.
- N. S. Singh, K. L. Habicht, R. Moaddel and R. Shimmo, J Chromatogr B Analyt Technol Biomed Life Sci, 2017, 1055-1056, 144-148.
- S. G. Wubshet, I. M. Brighente, R. Moaddel and D. Staerk, J Nat Prod, 2015, 78, 2657-2665.
- P. A. Bhatia, R. Moaddel and I. W. Wainer, *Talanta*, 2010, 81, 1477-1481.
- 13. R. Moaddel, H. K. Musyimi, M. Sanghvi, C. Bashore, C. R. Frazier, M. Khadeer, P. Bhatia and I. W. Wainer, *J Pharm Biomed Anal*, 2010, **52**, 416-419.
- M. Sanghvi, R. Moaddel, C. Frazier and I. W. Wainer, J Pharm Biomed Anal, 2010, 53, 777-780.
- C. Temporini, S. Ceruti, E. Calleri, S. Ferrario, R. Moaddel, M. P. Abbracchio and G. Massolini, *Anal Biochem*, 2009, 384, 123-129.
- R. H. Fang, C. M. Hu, B. T. Luk, W. Gao, J. A. Copp, Y. Tai, D.
 E. O'Connor and L. Zhang, Nano Lett, 2014, 14, 2181-2188.
- 17. P. Angsantikul, S. Thamphiwatana, W. Gao and L. Zhang, Vaccines (Basel), 2015, **3**, 814-828.
- 18. D. Bhowmik, K. R. Mote, C. M. MacLaughlin, N. Biswas, B. Chandra, J. K. Basu, G. C. Walker, P. K. Madhu and S. Maiti, *ACS Nano*, 2015, **9**, 9070-9077.
- 19. C. Gao, Z. Lin, B. Jurado-Sanchez, X. Lin, Z. Wu and Q. He, *Small*, 2016, **12**, 4056-4062.
- S. Kaosaar, A. Kahru, P. Mantecca and K. Kasemets, *Toxicol In Vitro*, 2016, 35, 149-162.
- 21. H. Zhou, Z. Fan, P. K. Lemons and H. Cheng, *Theranostics*, 2016, **6**, 1012-1022.

- L. Rao, L. L. Bu, B. Cai, J. H. Xu, A. Li, W. F. Zhang, Z. J. Sun,
 S. S. Guo, W. Liu, T. H. Wang and X. Z. Zhao, *Adv Mater*,
 2016, 28, 3460-3466.
- 23. A. Narain, S. Asawa, V. Chhabria and Y. Patil-Sen, Nanomedicine (Lond), 2017, 12, 2677-2692.
- Z. Chai, X. Hu, X. Wei, C. Zhan, L. Lu, K. Jiang, B. Su, H. Ruan,
 D. Ran, R. H. Fang, L. Zhang and W. Lu, *J Control Release*,
 2017, 264, 102-111.
- S. Y. Li, H. Cheng, W. X. Qiu, L. Zhang, S. S. Wan, J. Y. Zeng and X. Z. Zhang, *Biomaterials*, 2017, 142, 149-161.
- L. Wang, W. Dai, M. Yang, X. Wei, K. Ma, B. Song, P. Jia, Y. Gong, J. Yang and J. Zhao, Colloids Surf B Biointerfaces, 2018, 176, 1-8.
- V. Vijayan, S. Uthaman and I. K. Park, Adv Exp Med Biol, 2018, 1064, 45-59.
- G. Deng, Z. Sun, S. Li, X. Peng, W. Li, L. Zhou, Y. Ma, P. Gong and L. Cai, ACS Nano, 2018, DOI: 10.1021/acsnano.8b05292.
- J. Li, X. Wang, D. Zheng, X. Lin, Z. Wei, D. Zhang, Z. Li, Y. Zhang, M. Wu and X. Liu, Biomater Sci, 2018, 6, 1834-1845.
- R. Yang, J. Xu, L. Xu, X. Sun, Q. Chen, Y. Zhao, R. Peng and
 Z. Liu, ACS Nano, 2018, DOI: 10.1021/acsnano.7b09041.
- R. J. Bose, R. Paulmurugan, J. Moon, S. H. Lee and H. Park, *Drug Discov Today*, 2018, 23, 891-899.
- Y. Jiang, J. M. Fay, C. D. Poon, N. Vinod, Y. Zhao, K. Bullock,
 S. Qin, D. S. Manickam, X. Yi, W. A. Banks and A. V. Kabanov,
 Adv Funct Mater, 2018, 28.
- Z. Chen, F. Liu, Y. Chen, J. Liu, X. Wang, A. T. Chen, G. Deng,
 H. Zhang, J. Liu, Z. Hong and J. Zhou, Adv Funct Mater, 2017,
 27.
- 34. Y. Bu, Q. Hu, R. Ke, Y. Sui, X. Xie and S. Wang, *Chem Commun (Camb)*, 2018, **54**, 13427-13430.
- 35. Y. L. Xu, Y. Qin, S. Palchoudhury and Y. P. Bao, *Langmuir*, 2011, **27**, 8990-8997.
- J. Sherwood, Y. Xu, K. Lovas, Y. Qin and Y. Bao, Journal of Magnetism and Magnetic Materials, 2017, 427, 220-224.
- Y. Xu, D. C. Baiu, J. A. Sherwood, M. R. McElreath, Y. Qin, K.
 H. Lackey, M. Otto and Y. Bao, Journal of Materials Chemistry B, 2014, 2, 6198-6206.
- 38. H. B. Na, I. C. Song and T. Hyeon, *Journal*, 2009, **21**, 2133–2148.
- N. Lee and T. Hyeon, *Chemical Society Reviews*, 2012, 41, 2575-2589.
- T. Hyeon, S. S. Lee, J. Park, Y. Chung and H. B. Na, *Journal*, 2001, 123, 12798-12801.
- K. An, M. Park, J. H. Yu, H. B. Na, N. Lee, J. Park, S. H. Choi,
 I. C. Song, W. K. Moon and T. Hyeon, European Journal of Inorganic Chemistry, 2012, DOI: 10.1002/ejic.201101193, 2148-2155.
- 42. Y. P. Bao, T. L. Wen, A. C. S. Samia, A. Khandhar and K. M. Krishnan, *Journal of Materials Science*, 2016, **51**, 513-553.
- 43. Y. L. Xu, S. Palchoudhury, Y. Qin, T. Macher and Y. P. Bao, *Langmuir*, 2012, **28**, 8767-8772.
- B. T. Luk, C. M. J. Hu, R. N. H. Fang, D. Dehaini, C. Carpenter,
 W. W. Gao and L. F. Zhang, *Nanoscale*, 2014, 6, 2730-2737.
- 45. H. S. Jang, Molecules, 2017, 22.
- A. Stewart, Cold Spring Harb Protoc, 2018, 2018, pdb prot094037.
- D. Gundisch and C. Eibl, Expert Opin Ther Pat, 2011, 21, 1867-1896.